



Contents lists available at SciVerse ScienceDirect

Materials Science and Engineering A

journal homepage: www.elsevier.com/locate/msea

Experimental study on shear properties of porous metal fiber sintered sheet

Zhenping Wan^a, Bin Liu^a, Wei Zhou^{b,*}, Yong Tang^a, K.S. Hui^c, K.N. Hui^d^a School of Mechanical and Automotive Engineering, South China University of Technology, Guangzhou 510640, China^b School of Engineering, Sun Yat-sen University, Guangzhou 510006, China^c Department of Systems Engineering and Engineering Management, City University of Hong Kong, Hong Kong^d Department of Materials Science and Engineering, Pusan National University, Republic of Korea

ARTICLE INFO

Article history:

Received 20 December 2011

Received in revised form 7 February 2012

Accepted 14 February 2012

Available online 3 March 2012

Keywords:

Porous materials

Sintering

Shear properties

Microstructure

ABSTRACT

A novel porous metal fiber sintered sheet (PMFSS) with high porosity was fabricated by the solid-state sintering method of copper fibers. In this study, the shear experiments were conducted to investigate the effect of porosity and sintering parameter on the shear properties of PMFSS. The typical shear stress–strain plot of PMFSS was obtained based on a larger number of shear test results. The shear fracture process of PMFSS was then divided into three steps: linear elastic stage, plastic deformation stage, and shear fracture stage. The shear strength was found to be decreased with increasing porosity ranging from 70% to 90% when the PMFSS was produced under the same sintering parameter. Moreover, the influence of sintering parameter on shear strength of PMFSS was also investigated. Our experimental results showed that the increase of the sintering temperature or holding time would give rise to the increase of shear strength of PMFSS.

Crown Copyright © 2012 Published by Elsevier B.V. All rights reserved.

1. Introduction

Porous metals used as the structural and functional materials have received considerable attention due to interesting combinations of mechanical, thermal and physical properties [1,2]. Generally, porous metals with high porosity are always classified by the pore size and pore shape, including the metal foams and metal fiber porous materials. The porous metal fiber sintered sheet (PMFSS), a new type of porous metals, has a three-dimensional reticulated structure featuring high porosity and large specific surface area. In the factual engineering applications, the PMFSS has been widely used in the defense and military, petrochemical industry, metallurgical machinery, environmental protection for its excellent performance in filtration and separation [3], flow field and gas diffusion [4], energy absorption [5], biomedical device [6], catalytic reaction [7,8], heat transfer [9] and so on. With the extension of its application field and increasing complexity of its working environment, it is important to understand the relationship between structure and properties of PMFSS to widen its application. So far, the tensile and compressive properties of PMFSS fabricated using the stainless steel fibers and copper fibers have been comprehensively investigated via experimental observation and theoretical modeling in the literatures [10–12]. However, the

relationship between microscopic structures and shear properties of PMFSS is not understood well.

In recent years, we found that the number of research works dealing with the mechanical properties of metal foam increased significantly, such as copper foam [13,14], aluminum foam [15,16], steel foam [17] and other metal foams [18]. These results provide the effective guideline to improve the design and manufacturing methods of metal foam for engineering application. However, there is limited information about the shear properties of metal foams. Von Hagen and Bleck [19] carried out the experimental study on the compressive, tensile and shear properties of aluminum foams. The shear strength of aluminum foams was found to increase linearly with increasing density. Saenza et al. [20] studied the effect of cell size distribution on the shear properties of aluminum foam produced using AlSi7Mg and SiC particles. Besides, Wang et al. [21] obtained the tensile and shear behaviors of closed cell Al foams, according to ASTM standards. It was further found that these behaviors differed from those in compression.

Recently, although there is increasing research works about the new manufacturing method for PMFSS, only a little attention was given to the study on the microscopic structures and shear properties of PMFSS. Clyne and Markaki [22,23] produced highly porous sheets using liquid phase sintering of short stainless steel fibers with a diameter of 100 μm. They found that the sheets have a porosity varied from 75% to 95% and a tensile strength below 1 MPa. Liu et al. [24] developed a new porous steel wire mesh with open porosities prepared by the metallurgical route. The effects of the forming pressure and sintering parameters on the porous structure

* Corresponding author. Tel.: +86 20 39332148; fax: +86 20 39332148.

E-mail addresses: zhouw23@mail.sysu.edu.cn, abczhoulin@163.com (W. Zhou).

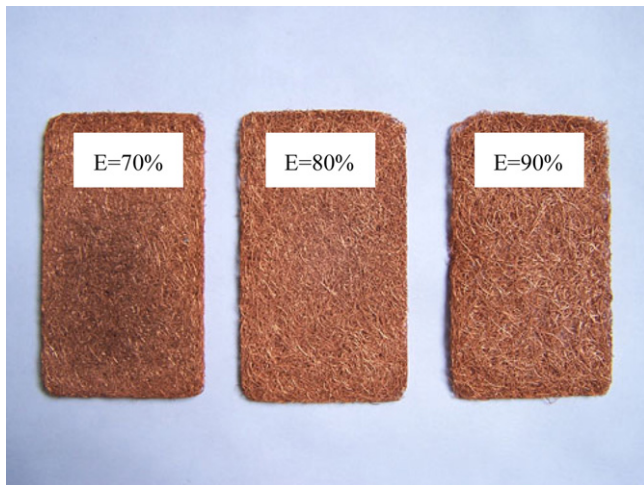


Fig. 1. Appearance of PMFSS with different porosities produced by the solid-state sintering of copper fibers.

and compressive properties were discussed. Moreover, Wang et al. [25] fabricated a PMFSS using the vacuum sintering of stainless steel fibers with a diameter of 100 μm , studying the shear properties of PMFSS with porosity range from 70% to 95%.

From the above reported work, it is found that the detailed study of the shear properties of PMFSS using the copper fibers is lacking in current literatures. This paper investigates the shear fracture process of PMFSS produced by solid-state sintering of copper fibers. After examining the microstructures, the shear properties of PMFSS is further analyzed and discussed by varying the porosity and sintering parameter.

2. Experimental procedure

2.1. Manufacturing process of PMFSS

As reported previously [26], the processing procedure of PMFSS was divided into the following five steps: fiber chipping, mold-pressing, sintering, cooling and testing. First of all, the continuous copper fibers were fabricated by cutting method with a multi-tooth tool. These copper fibers were then cut into segments with the length ranging from 10 to 20 mm. Next, the copper fibers with random directions were uniformly put into the packing chamber of the mold pressing equipment and then pressure was applied by screwing the bolts. In this way, the semi-finished PMFSS with the same shape as the predetermined packing chamber was obtained. Sintering was carried out in the box-type furnace which provided the hydrogen gas atmosphere with constant pressure of 0.3 MPa. The sintering temperature was in the range from 700 $^{\circ}\text{C}$ to 1000 $^{\circ}\text{C}$ and controlled by a programmable temperature controller. Stage heating method was used to optimize the heating rate. The heating rate was kept at 300 $^{\circ}\text{C}/\text{h}$ when the temperature was below 800 $^{\circ}\text{C}$, while reduced to 200 $^{\circ}\text{C}/\text{h}$ as the temperature raised above 800 $^{\circ}\text{C}$. The holding time was set as 30 min, 60 min, or 90 min. When the sintering was completed, the sample was removed from the furnace and cooled in air to room temperature. Finally, the mold pressing equipment was disassembled and the PMFSS was ready for shear measurement. The appearance of PMFSS with different porosities produced by above manufacturing procedure is shown in Fig. 1.

Since the obtained PMFSS has a regular geometric shape, we can calculate the average porosity using the quality-volume method formulated by

$$\theta (\%) = \left(1 - \frac{M}{\rho V} \right) \times 100 \quad (1)$$

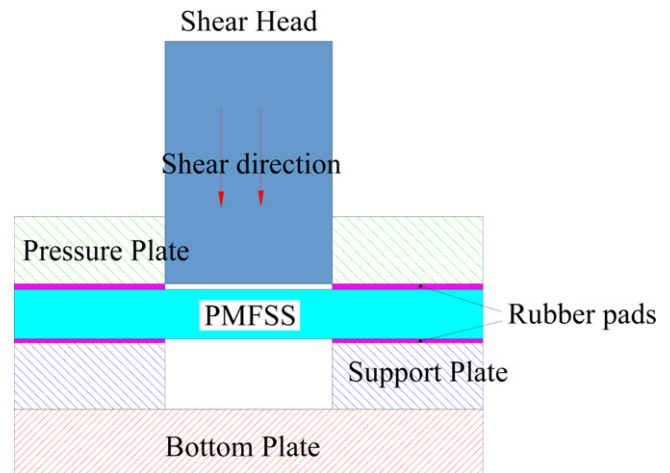


Fig. 2. Schematic diagram of shear test device for measuring the shear properties of PMFSS.

where V is the volume of PMFSS (cm^3), M is the mass of PMFSS (g), and ρ is the density of red copper (g/cm^3).

2.2. Shear test of PMFSS

The shear test was carried out on a PC-controlled electronics universal testing machine (RGL-20A) with maximum load of 20 kN, performing both test control and data acquisition. To avoid the size effect, the minimal length, width and height of samples are required to be at least seven times larger than the pore size [27]. The dimension of PMFSS was designed to be 70 mm in length, 40 mm in width, and 2 mm in height, as shown in Fig. 1. To study the shear properties of PMFSS, a shear test device need to be designed according to the shear test standard [28], as shown in Fig. 2. Before the shear test, the PMFSS was positioned on two support plates with a spacing of 30 mm and then was clamped with two pressure plates. Both the pressure plates and the support plates were protected with rubber pads to avoid the deformation and destruction of the reticulated structure in the clamping process. The shear procedure of all test samples was conducted at a constant shear rate of 1.5 mm/min using the shearing head, which was automatically controlled by the computer software. During each test the load and displacement were recorded continuously to failure. The stress was calculated from the load and the initial section of the sample, whereas the strain was obtained from the displacement of shearing head and the initial measured height of sample [29]. The maximum stress in the stress-strain plots was determined as the shear strength of PMFSS. To get the accurate value of shear strength, five specimens were tested in each case and an average was taken. All the shear tests were performed at room temperature (approximately 25 $^{\circ}\text{C}$). Moreover, the microscopic morphology of PMFSS was observed using a scanning electron microscopy (JSM-6380LA, Japan).

3. Results and discussion

3.1. Microstructural characterization

Before sintering procedure, the copper fibers were distributed randomly into the pressing mold. The pressurization was conducted to produce the mesh structure with many contact regions among fibers. In the sintering process, the sintering joints between fibers were formed under the setting temperature as a result of material migration, and then fiber's metallurgy unification happened. Finally, the PMFSS with three-dimensional reticulated structure was obtained. The SEM image of PMFSS with typical

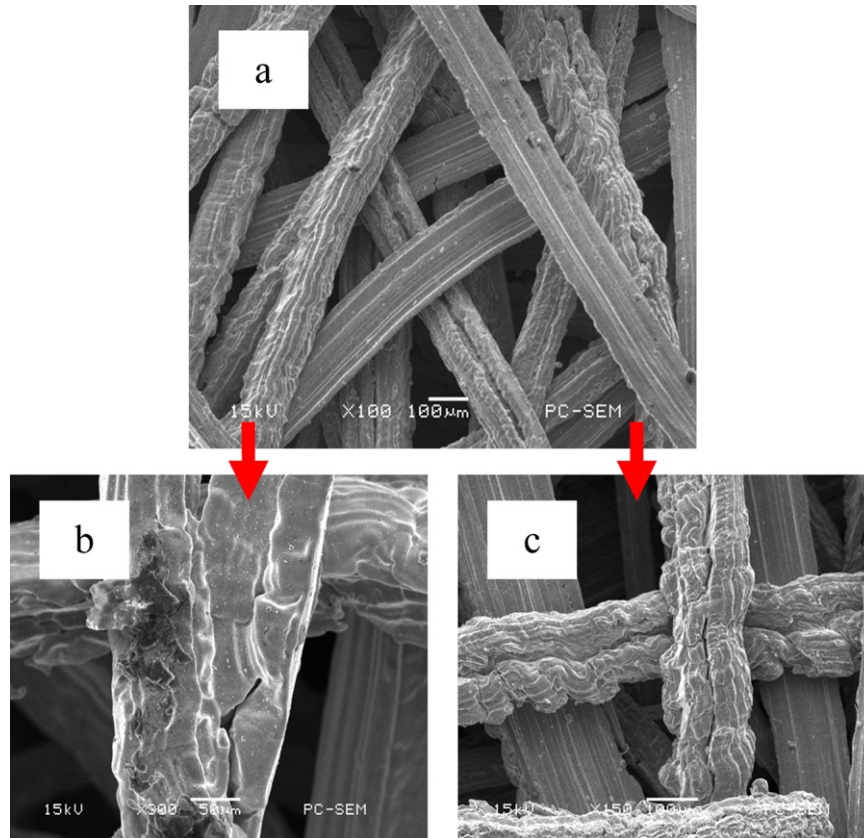


Fig. 3. SEM images of PMFSS produced by the solid-state sintering of copper fibers. (a) Typical three-dimensional reticulated structure of PMFSS; bonding types among fibers in the PMFSS: (b) fiber-to-fiber surface contact, (c) crossing fiber meshing.

three-dimensional reticulated structure is shown in Fig. 3a. Besides, further investigation shows that many mountain-like microstructures within micro/nanometer scale were also found on the surface of copper fibers in the PMFSS before and after sintering [26]. The experimental results indicated that these microstructures created many contact joints to carry out the sintering process, resulting in the strength enhance of sintering joints. Moreover, we found that there were two kinds of sintering joints in the PMFSS including fiber-to-fiber surface contact and crossing fiber meshing, as shown in Fig. 3b and c, respectively [26]. These sintering joints favor to improve the mechanical properties of PMFSS. It was also noted that the PMFSS had a wide porosity range from 60% to 98%, large pore size and interconnected pores. In addition, the mechanical properties of PMFSS with three-dimensional reticulated structure can be tailored for different applications by varying the sintering parameters for PMFSS.

3.2. Shear fracture process of PMFSS

Fig. 4 shows the shear stress–strain plots of PMFSS with 80% porosity sintered at 900 °C for 30 min. From this plot, the shear fracture process of PMFSS can be easily divided into the following three distinct stages: (a) initial linear elastic stage, (b) plastic deformation stage of three dimensional reticulated structure and neighboring fiber, and (c) shear fracture stage of the overall three dimensional reticulated structure. These three stages correspond to OA, AB and BC, respectively, as shown in Fig. 4. The similar three stages of shear properties were also found in the shear stress–strain plot for the stainless steel fiber porous materials [25]. In the initial shear stage, only short-term elastic deformation occurred in this stage. It was found that the stress linearly increased with increasing strain according to the linear elastic Hooke's law. Meanwhile,

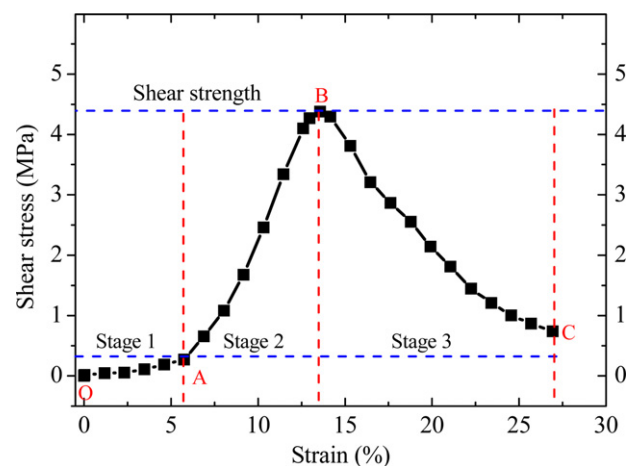


Fig. 4. Typical shear stress–strain plot of PMFSS with 80% porosity sintered at 900 °C for 30 min.

the three-dimensional reticulated structure of PMFSS experienced little deformation and orientation-changes along the shear direction. After the elastic stage, the local stress was increased greatly due to the plastic deformation of three dimensional reticulated structures and neighboring fiber's yielding as well as plastic deformation. When the shear stress was increased to the ultimate value, the sintering joints and fiber filaments in the PMFSS began to irreversibly deform and fracture, quickly leading to the destruction of the entire reticulated structure. So, the stress–strain plot presented a sharp drop stage. Comparing to the other metal foams [20], the shear failure strain was higher than 10%, thus the PMFSS exhibited a good plastical behavior. After the shear testing, the SEM image

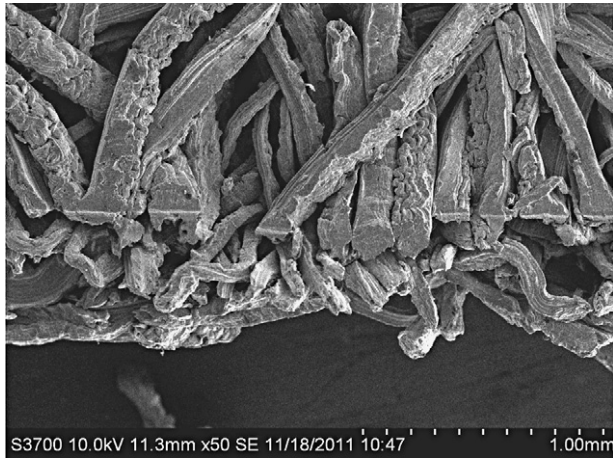


Fig. 5. SEM image of cross-section of PMFSS after shear test. Sample was sintered at 900 °C for 30 min.

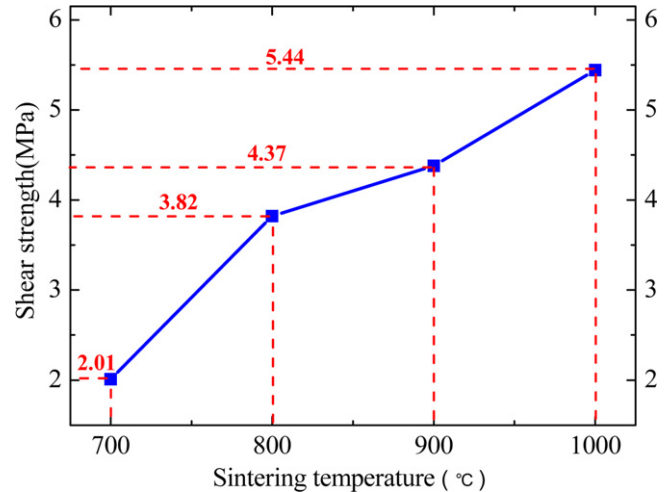


Fig. 7. Shear strength plot of PMFSS with 80% porosity sintered at different temperatures for 30 min.

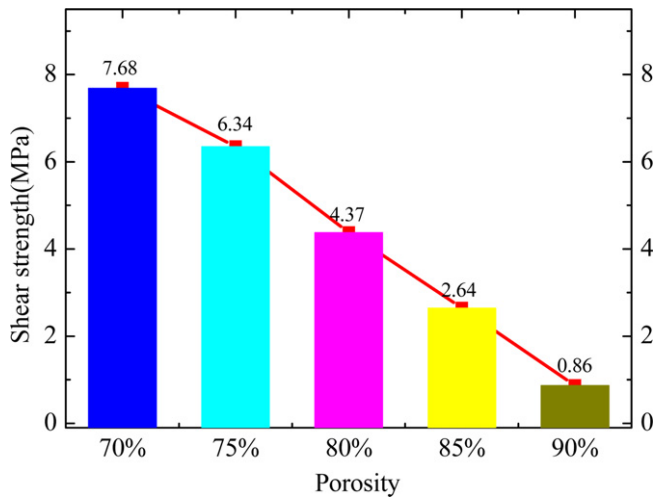


Fig. 6. Shear strength plot of PMFSS sintered at 900 °C for 30 min with different porosities.

of cross-section of PMFSS sintered at 900 °C for 30 min is shown in Fig. 5. The initial shear edge was easily found on the surface of PMFSS. Moreover, the single damaged and fractured copper fibers exhibited different lengths in the PMFSS as a result of unique three dimensional reticulated structure.

3.3. Effect of porosity on the shear strength of PMFSS

Porosity, as the most intrinsic feature of porous materials, plays an important role in determining the mechanical properties of PMFSS [30]. In this study, the effect of porosity on the shear strength of PMFSS was investigated using five porosities of 70%, 75%, 80%, 85% and 90%. Fig. 6 shows the shear strength of PMFSS with different porosities sintered at 900 °C for 30 min. The results indicated that the significant influence of porosity on the shear strength of PMFSS was observed. The shear strength of PMFSS with 70% porosity was about 7.68 MPa. However, the shear strength was decreased to 0.86 MPa when the porosity was increased to 90%. These results are attributed to the change of effective shear cross section for the PMFSS with different porosities. For the PMFSS with low porosity, the shear cross section will include larger number of copper fibers. Furthermore, the larger number of copper fibers also leads to produce more sintering joints in the sintering process. Therefore, these

results will help to improve the shear strength of PMFSS with low porosity.

3.4. Effect of sintering parameters on the shear strength of PMFSS

3.4.1. Sintering temperature

Four samples with 80% porosity sintered at 700 °C, 800 °C, 900 °C and 1000 °C for 30 min were selected to investigate the influence of sintering temperature on the shear strength of PMFSS. Fig. 7 shows the shear strength plot of PMFSS samples sintered at different temperatures. It was clear that the shear strength of PMFSS linearly increased with the increase of the sintering temperature. When the sintering temperature was increased to 1000 °C, the shear strength was increased to 5.44 MPa. The shear strength showed the higher value than that of sintering stainless steel material with the same porosity [25]. This maybe attributed that the higher sintering temperature is beneficial for the atom diffusion to accelerate the sintering process. Sintering joints then will be coarsen and the contact interfaces among fibers are increased [12,26], resulting in higher shear strength. Thus, in the sintering temperature range from 700 °C to 1000 °C, the shear strength can be improved by the increase of sintering temperature to satisfy with different demands.

3.4.2. Holding time

The shear strength values of PMFSS samples with 80% porosity sintered at 900 °C and 1000 °C for different holding times are shown in Fig. 8. It was found that the shear strength of PMFSS sintered at 900 °C was increased from 4.3 MPa to 5.7 MPa when the holding time was extended from 30 min to 90 min. We concluded that the shear strengths of PMFSS slightly increased with increasing holding time. The similar law was also found for the PMFSS sintered at 1000 °C for different holding times. For longer holding time, the coarser sintering joints among fibers are easily produced [24,26]. So the shear strength of PMFSS is improved under the longer holding time. However, the increase of sintering time also caused the coarser grain in copper fiber [24], resulting in the decrease of single fiber's shear strength. Then the shear properties of PMFSS will be decreased under longer holding time. Thus, the combination of these behaviors will lead to the slight increase of shear strength with increasing holding time. In the engineering applications, the shear properties of PMFSS can be tailored by varying the sintering temperature and holding time.

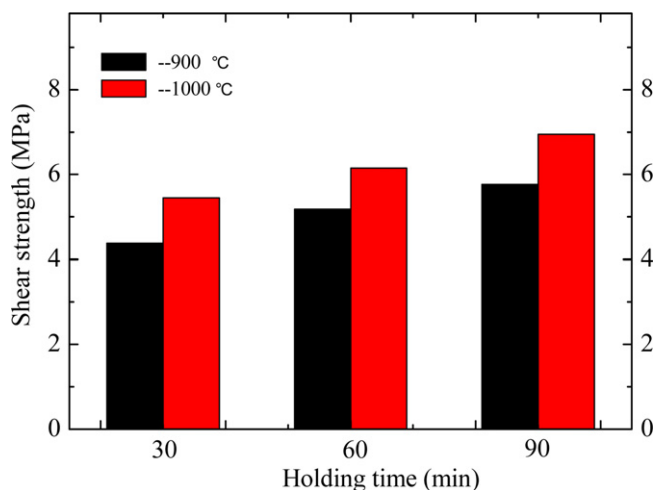


Fig. 8. Shear strength values of PMFSS with 80% porosity sintered at 900 °C and 1000 °C for different holding times.

4. Conclusions

The shear test was conducted to investigate the shear properties of PMFSS produced by the solid-state sintering process. The PMFSS with a three-dimensional reticulated structure exhibited the unique properties in the shear failure process. The shear fracture process of PMFSS included the following three steps: initial linear elastic stage, plastic deformation stage of three dimensional reticulated structure and neighboring fiber, as well as shear fracture stage of the overall three dimensional reticulated structure. Moreover, the porosity and sintering parameter were changed to study on the shear strength of PMFSS. Our experimental results indicated the porosity affected the shear strength of PMFSS greatly. Higher shear strength of PMFSS was obtained when porosity was decreased. Besides, the sintering parameters also play important roles in determining the shear strength of PMFSS. The shear strength of PMFSS was linearly increased with the increase of the sintering temperature in the range of 700–1000 °C. Moreover, the holding time also could slightly affect the shear strength due to change of the microstructures of PMFSS. These results obtained in this work will not only help to further develop the porous fiber materials, but also provide an important technical guideline to widen the potential application of PMFSS.

Acknowledgements

The research work was supported by the National Nature Science Foundations of China (No. 51105387, No. U0934005 and No. 51075155), Natural Science Foundation of Guangdong Province (No. S2011040002152). The support from the Foundation of Key Laboratory of Surface Functional Structure Manufacturing of Guangdong Higher Education Institutes at the South China University of Technology (No. SFS-KF201009) is also acknowledged.

References

- [1] J. Banhart, *Prog. Mater. Sci.* 46 (2001) 559–632.
- [2] L.P. Lefebvre, J. Banhart, D.C. Dunand, *Adv. Eng. Mater.* 10 (2008) 775–787.
- [3] A. Nabovati, E.W. Llewellyn, A.C.M. Sousa, *Compos. A* 40 (2009) 860–869.
- [4] J.K. Kuo, C.K. Chen, *J. Power Sources* 162 (2006) 207–214.
- [5] B. Zhang, T.N. Chen, *Appl. Acoust.* 70 (2009) 337–346.
- [6] G. Ryan, A. Pandit, D.P. Apatsidis, *Biomaterials* 27 (2006) 2651–2670.
- [7] I. Yuranov, L. Kiwi-Minsker, A. Renken, *Appl. Catal. B – Environ.* 43 (2003) 217–227.
- [8] Y. Tang, W. Zhou, M.Q. Pan, H.Q. Chen, W.Y. Liu, H. Yu, *Int. J. Hydrogen Energy* 33 (2008) 2950–2956.
- [9] A.S. Abduljalil, Z.B. Yu, A.J. Jaworski, *Mater. Des.* 32 (2011) 217–228.
- [10] P. Liu, G. He, L.H. Wu, *Mater. Sci. Eng. A* 509 (2009) 69–75.
- [11] J.C. Qiao, Z.P. Xi, H.P. Tang, J.Y. Wang, J.L. Zhu, *Rare Met. Mater. Eng.* 37 (2008) 2173–2176.
- [12] W. Zhou, Y. Tang, M.Q. Pan, X.L. Wei, J.H. Xiang, *Mater. Sci. Eng. A* 525 (2009) 133–137.
- [13] S.K. Hyun, H. Nakajima, *Mater. Sci. Eng. A* 340 (2003) 258–264.
- [14] A.M. El-Hadek, S. Kaytbay, *Int. J. Mech. Mater. Des.* 4 (2008) 63–69.
- [15] E. Koza, M. Leonowicz, S. Wojciechowski, F. Simancik, *Mater. Lett.* 58 (2003) 132–135.
- [16] A.H. Brothers, D.C. Dunand, *Mater. Sci. Eng. A* 489 (2008) 439–443.
- [17] N. Chawla, X. Deng, *Mater. Sci. Eng. A* 390 (2005) 98–112.
- [18] P.S. Liu, *Mater. Des.* 31 (2010) 2264–2269.
- [19] H. Von Hagen, W. Bleck, *Mater. Res. Soc. Symp. Proc.* 521 (1998) 59–64.
- [20] E. Saenza, P.S. Baranda, J. Bonhomme, *Mater. Res. Soc. Symp. Proc.* 521 (1998) 83–89.
- [21] X.Z. Wang, L.Z. Wu, S.X. Wang, *Mater. Technol.* 24 (2009) 161–165.
- [22] A.E. Markaki, V. Gergely, A. Cockburn, T.W. Clyne, *Compos. Sci. Technol.* 63 (2003) 2345–2351.
- [23] T.W. Clyne, A.E. Markaki, J.C. Tan, *Compos. Sci. Technol.* 65 (2005) 2492–2499.
- [24] P. Liu, G. He, L.H. Wu, *Mater. Sci. Eng. A* 489 (2008) 21–28.
- [25] J.Y. Wang, H.P. Tang, J.L. Zhu, J.C. Qiao, Z.P. Xi, C.Y. Zang, Q.B. Ao, C. Li, *J. Funct. Mater.* 41 (2010) 565–567.
- [26] Y. Tang, W. Zhou, J.H. Xiang, W.Y. Liu, M.Q. Pan, *Mater. Manuf. Process.* 25 (2010) 565–571.
- [27] M.F. Ashby, T. Evans, N.A. Fleck, L.J. Gibson, J.W. Hutchinson, H.N.G. Wadley, *Metal Foams: A Design Guide*, Butterworth-Heinemann, Woburn, MA, 2000.
- [28] Z.P. Xi, H.P. Tang, J.Y. Wang, Y.J. Wu, L.F. Dong, B.J. Yang, *Rare Met. Mater. Eng.* 36 (2007) 555–558.
- [29] L. Peroni, M. Avalle, M. Peroni, *Int. J. Impact Eng.* 35 (2008) 644–658.
- [30] P.S. Liu, T.F. Li, C. Fu, *Mater. Sci. Eng. A* 268 (1999) 208–215.